

Neuroprotective Properties of Inhaled Argon-Oxygen Mixture after Photochemically Induced Ischemic Stroke

Ekaterina A. Boeva^{1*}, Maxim V. Sutormin¹, Artem N. Kuzovlev¹,
Maxim A. Lyubomudrov¹, Victor V. Moroz¹, Natalia I. Usoltseva¹, Oleg A. Grebenchikov¹

¹ V. A. Negovsky Research Institute of General Reanimatology,
Federal Research and Clinical Center of Intensive Care Medicine and Rehabilitology,
25 Petrovka Str., Bldg. 2, 107031 Moscow, Russia

² M. F. Vladimirsky Moscow Regional Research Clinical Institute
61/2 Shchepkin Str., 129110 Moscow, Russia

For citation: Anastasia M. Tynterova, Ekaterina M. Moiseeva, Matvey S. Khoymov, Natalya N. Shusharina. Predictive Markers of Functional Outcome in Subtypes of Ischemic Stroke. *Obshchaya Reanimatologiya = General Reanimatology*. 2025; 21 (5): 35–43. <https://doi.org/10.15360/1813-9779-2025-5-2525> [In Russ. and Engl.]

*Correspondence to: Ekaterina A. Boeva, eboeva@fnkcr.ru

Summary

The aim of this study was to investigate the effects of three 60-minute inhalations of an argon-oxygen gas mixture (Ar 70%/O₂ 30%) on the severity of neurological deficits, brain lesion volume, inflammatory and cellular responses, and cytokine levels in rats after photochemically induced ischemic stroke.

Materials and Methods. The experiment was performed in 21 male Wistar rats (250–300 g) randomly assigned to three groups: (1) ischemia + N₂ 70%/O₂ 30% inhalation (ischemia group, *N*=10); (2) ischemia + Ar 70%/O₂ 30% inhalation (ischemia + iAr group, *N*=8); and (3) sham-operated animals (sham group, *N*=3). Neurological status was assessed over 14 days using the limb placement test. On day 14 post-ischemia, animals underwent magnetic resonance imaging (MRI), histological and immunohistochemical analyses, and RT-PCR using RNA extracted from the liquid homogenate of the entire brain to evaluate the relative levels of IL-1 β , IL-6, and TNF mRNAs.

Results. Significant differences in limb placement test scores were observed between ischemia and ischemia + iAr groups on day 3 (7.3 [5.3; 10.4] vs. 9.9 [10.2; 13.2], *P*=0.045) and day 7 (8.0 [7.3; 9.2] vs. 10.0 [9.0; 11.5], *P*=0.027). MRI showed a significantly smaller ischemia volume in the ischemia + iAr group compared to the ischemia group (12.5 [8.5; 17.4] mm³ vs. 21.0 [17.5; 22.68] mm³, *P*=0.01). Pro-inflammatory cytokine levels were significantly lower following argon-oxygen inhalation: IL-1 β — 205 [175.5; 247.5] in the Ischemia + iAr group vs. 328.5 [299; 347.5] in the Ischemia group (*P*=0.001); TNF — 110.5 [93.5; 113] vs. 149.5 [126.5; 176.5], respectively (*P*=0.001).

Conclusion. Repeated 60 min inhalation of argon-oxygen mixture (Ar 70%/O₂ 30%) after photochemically induced ischemic stroke significantly reduces neurological impairment, modulates pro-inflammatory cytokine levels, and affects inflammatory and cellular responses.

Keywords: argon; ischemia; neuroprotection; photochemically induced stroke

Conflict of interest. The authors declare no conflict of interest.

Information about the authors/Информация об авторах:

Ekaterina A. Boeva/Екатерина Александровна Боева: <http://orcid.org/0000-0002-0422-5018>

Maxim V. Sutormin/Максим Викторович Сутормин: <http://orcid.org/0009-0001-5563-0363>

Artem N. Kuzovlev/Артём Николаевич Кузовлев: <https://orcid.org/0000-0002-5930-0118>

Maxim A. Lyubomudrov/Максим Алексеевич Любомудров: <https://orcid.org/0000-0002-1735-592X>

Victor V. Moroz/Виктор Васильевич Мороз: <https://orcid.org/0000-0002-5030-5457>

Natalia I. Usoltseva/Наталья Ивановна Усольцева: <http://orcid.org/0000-0002-7269-6444>

Oleg A. Grebenchikov/Олег Александрович Гребенчиков: <https://orcid.org/0000-0001-9045-6017>

Introduction

Stroke is a significant cause of morbidity and mortality. Multitudinous studies of stroke have been conducted, however, therapeutic options for patients remain limited [1]. Extensive research of ischemic stroke pathogenesis has shown that neuronal damage is caused by neuronal death, oxidative stress, and diverse immune responses [2–4]. The repair of neuronal damage caused by ischemic stroke involves various molecular pathways. Neuronal survival provides the stability and completeness of brain functions, and neuronal loss directly leads to neurological

deficits [5–10]. Therefore, ensuring the protection and regeneration of neurons is a crucial step in effective recovering from neurological deficits. In addition, cellular responses involving expression of pro-inflammatory mediators provide the base for ischemic tissue damage [7, 8, 10]. It is widely recognized that targeted activation of microglia and resident immune cells of the central nervous system can inhibit damage and promote recovery after stroke. Excessive activation of the phagocytic phenotype of microglia leads to exacerbation of brain damage due to phagocytosis of still viable cells. Mi-

croglia with a phagocytic phenotype releases pro-inflammatory cytokines, which also exacerbates the damage. At the same time, microglia of the restorative phenotype release trophic and anti-inflammatory factors. This indicates that microglia are characterized by great heterogeneity [7, 8, 10]. Cellular reactions involving expression of pro-inflammatory mediators at the blood-endothelium interface, such as adhesion molecules, cytokines, chemokines, and leukocytes, significantly contribute to the pathogenesis of tissue damage in ischemic stroke [11, 13, 14]. Interleukins also play an important role in the development of ischemic stroke [11]. Interleukins are the cytokines. to regulate and mediate inflammatory and immune responses, and hematopoiesis [12]. They play a crucial role in the processes of information transfer, activation and regulation of immune cells, mediating the activation, proliferation, and differentiation of T and B cells, as well as the cellular responses involving expression of pro-inflammatory mediators [11–13]. In particular, IL-1 β stimulates activation of microglia, the main effector cells in cellular response, leading to secondary brain damage through stimulation of secretion and release of potentially neurotoxic molecules, such as TNF- α and iNOS [11–15].

The development of neuroprotective compounds is an urgent task for modern science. Argon represents one of promising candidate molecules as a potential neuroprotector [16–18].

The results of studies of various neuroprotective agents are contradictory. The potency of neuroprotective effect depends on the model used, the exposure time, and the anesthetic agent itself [16–18]. In this regard, the aim of this study was to establish whether an argon-oxygen mixture has a neuroprotective effect after three 60-minute inhalations following a photo-induced ischemic stroke, as well as to find out how the proposed inhalation technique affects the cellular response of the brain.

Material and Methods

The experiments were conducted on male Wistar rats weighing 250–300 g ($N=21$). Eight hours before the experiment, the animals were deprived of food, but they still had access to water. The study protocol was approved by the Local Ethics Committee of the Federal Scientific and Clinical Center for Intensive Care Medicine and Rehabilitology (No. 3/22/3 dated December 14, 2022). All experiments were conducted in accordance with Directive 2010/63/EU of the European Parliament and of the Council of the European Union on the protection of animals used in scientific research.

The rats were randomly assigned to three groups depending on the interventions:

— the control group included animals with ischemia receiving inhalation with a gas mixture of N₂ 70%/O₂ 30% (ischemia group, $N=10$);

— the experimental group included animals with ischemia and inhalation of Ar 70%/O₂ 30% gas mixture (ischemia + iAr group, $N=8$);

— the sham-operated group included animals without ischemia and no anesthesia and gas inhalation (SO group, $N=3$).

Modeling of photo-induced ischemic stroke.

The stroke model was reproduced using the standard method [19], and 6% chloral hydrate (300 mg/kg, intraperitoneal) was used as the anesthetic agent. Approximately 42 \pm 16 minutes after the onset of the stroke, when the animal regained consciousness and restored its thermoregulation, it was anesthetized (paracetamol 50 mg/kg, subcutaneously) and placed in the chamber. A fresh gas mixture was constantly supplied to the chamber at a flow rate of 3 L/min (at least 0.5 L/min per animal): for the Ischemia group, oxygen-air (O₂ 30%), and for the Ischemia + iAr group, Ar 70%/O₂ 30%. Standard wood shavings on chamber bottom were used for drainage of liquids. The animal remained in the chamber for 60 minutes. After this period, the animal's overall condition (alertness and mobility) was assessed, the animal was re-anesthetized with paracetamol (50 mg/kg, subcutaneously) and placed in a cage with access to water and food. O₂ and CO₂ levels in the chamber were continuously monitored throughout the experiment, using a multi-gas sensor from InertGas Medical LLC. After 24 hours, the rats were again exposed to inhalation for 60 minutes, the next procedure was performed 72 hours after the start of the experiment. The study used a gas mixture produced by AKELA-N LLC, Khimki, Russia.

Assessment of neurological status. In this study the Limb Placement Test (LPT) was used, following a protocol based on M. De Rieck et al. methodology [20], modified by Y. Yolkkonen et al. [21].

Assessment of brain damage. Brain MRI using a 7 T magnetic field and a 105 mT/m gradient system (BioSpec 70/30, Bruker, Germany) was performed in animals 14 days after induction of stroke. Anesthesia was provided with isoflurane (1.5–2 vol %). A standard rat brain imaging protocol was used, including T2-weighted images. Spin echo-based (RARE) pulse sequences (PS) were used with the following parameters: TR=6000 ms, TE=63.9 ms, slice thickness 0.8 mm, slice spacing step 0.8 mm, 256 \times 384 matrix, resolution 0.164 \times 0.164 mm/pixel. The scanning time for one animal was approximately 25 min. To analyze the extent of brain damage, we used graphical image analysis in the ImageJ program (National Institutes of Health image software, Bethesda, MD, USA). For this purpose, the area of intact tissue in the healthy (S1) and damaged (S2) hemispheres was determined separately, and the area of damage was calculated using the formula $\Sigma S = S1 - S2$, where ΣS is the area of damage on one section (mm²). The volume of brain damage was calculated using the formula $V = \Sigma S_n \times d$, where d is the slice thickness

(0.8 mm), and ΣSn is the sum of brain damage areas on all sections (mm²).

Histological and immunohistochemical examination. For histological analysis on the 14th day after stroke brain samples were extracted from rats immediately after euthanasia (decapitation under chloral hydrate anesthesia) and fixed in 10% buffered formalin for 24 hours and then processed using standard paraffin techniques. Frontal sections 4 μ m thick were stained with hematoxylin and eosin and Nissl's stain. Morphometric analysis was performed after creating digital images using a Nikon Eclipse Ni-U microscope (Japan) with $\times 4$, $\times 10$, $\times 20$, $\times 40$ lenses and a DS-RI2 camera. Measurements were performed using the NIS-Elements BR software from Nikon (Japan), analyzing morphological changes and determining the area of damage in the infarct zone and penumbra.

The sections were then deparaffinized in xylene and rehydrated through a series of ethanol solutions. High-temperature antigen retrieval was performed in a citrate buffer with a pH of 6 (Target Retrieval Solution, DAKO, Denmark). The cooled sections were washed three times in a phosphate buffer (PBS IHC Wash Buffer + Tween, Cell Marque, USA) for 5 minutes. Endogenous peroxidase was blocked with 3% hydrogen peroxide for 10 min, and Protein Block Serum-free (Abcam, UK) was used for 30 min to prevent non-specific antibody binding. The sections were then incubated at 37°C for one hour with one of following primary antibodies: rabbit Iba-1 (ab153696, 1:500) for microglia, Rabbit NeuN (ab177487, 1:200) for neurons, Anti-Caspase-3 (ab13847, 1:100) for apoptosis, and rabbit anti-Von Willebrand factor (ab 9378, 1:200) for angiogenesis, all diluted in Antibody Diluent (ab64211 Abcam, Great Britain). Secondary goat anti-rabbit/mouse antibodies Dako REAL EnVision Detection System (DAB Dako Antibody Diluent) or ImmPACT[®] Vector[®] Red Substrate Kit, Alkaline Phosphatase (AP) (SK-5105) were then employed as recommended by the manufacturer. The sections were stained with hematoxylin for 1–2 min, then sequentially dehydrated in 70, 96, and 100% alcohol, and cleared twice in xylene.

Extraction of RNA from animal brain tissue.

RNA was extracted using the RNeasy MiniKit (QIAGEN, USA) according to the manufacturer's instructions. The entire brain of an animal weighing 25 mg was ground in liquid nitrogen using a pestle and mortar. 600 μ L of RLT buffer (QIAGEN, USA) was added to the resulting homogenate, and was homogenized using a syringe with a 0.8 mm needle. The resulting lysate was centrifuged for 3 min at 16100 g, then, the supernatant was transferred to a new tube. 450 μ L of 96% ethanol was added to it, and the solution was applied to the RNeasy column. To purify the RNA, the column was washed with 700 μ L of RW1 buffer and 500 μ L of RPE buffer twice. Elution

was performed using 50 μ L of RNase-free water. The eluted RNA was precipitated with the addition of sodium acetate (1/10 volume of 3M solution) and 96% ethanol (2.5 volumes), and then dissolved in 30 μ L of deionized water without RNAs.

Reverse transcription and real-time PCR. Reverse transcription was performed using the SuperScript III kit from ThermoScientific (USA). A mixture of oligo (dT)18 (500 μ g/ml) and 50 ng of random primers was prepared in a 1:1 ratio (1 μ L), and 2 μ g of total RNA, 1 μ L of deoxyribonucleotide mixture (10 μ M), and MQ were added to a volume of 12 μ L. The mixture was heated at 65°C for 6 min and cooled on ice. Then, 4 μ L of 5x-buffer, 2 μ L of 0.1M DTT, 1 μ L of reverse transcriptase (20 units), and 1 μ L of MQ were added. The mixture was incubated at room temperature for 10 minutes to anneal the random primers, then at 43°C for 50 minutes, after which the reaction was terminated by heating to 70°C for 15 minutes for enzyme inactivation.

The Beacon Designer program was used to select primers for PCR, and the appropriate primer pairs were selected for analysis (Table 1). According to the conditions specified in Table 2, real-time PCR was performed in a BioRad iCycler amplifier (USA) with a mixture of the following composition: Mixture B (intercalating dye Eva Green + recessive dye ROX + Taq Pol + 25mM dNTP + buffer (provided by Sintol) — 10 μ L, primers (mixture of 10 μ M forward and reverse primers — 0.5 μ L, MQ — 9.5 μ L, reverse transcription product — 5 μ L). During statistical processing the expression analysis results were normalized to the expression of the 18S rRNA gene. Statistical analysis was performed using GraphPad Prism 8.0 software. The normality of variable distribution in the samples was assessed using the Shapiro–Wilk test. In the case of normal distribution, the data were presented as the mean value and standard deviation; in the case of non-normal distribution, the data were presented as the median and interquartile range *Me* [*Q1*; *Q3*]. The nonparametric Mann-Whitney *U* test was used to assess the difference between two groups in the presence of at least one sample with a non-normal distribution. To compare more than two groups, the Kruskal–Wallis test was used with a post hoc analysis using Dunn's criterion. In this case, the adjustment for multiple comparisons (Dunn's multiple comparisons test) was taken into account. A two-tailed significance level was used in all tests. Differences were considered statistically significant at $P < 0.05$.

Results and Discussion

The limb placement test (LPT). No animals were withdrawn from the study for 14 days and no humane endpoint was reached. There were no lethal outcomes. When comparing the experimental groups with the SO group, the total LPT scores at each stage of the study were lower in the experimental

groups. Statistically significant differences were obtained between the Ischemia group and the Ischemia + iAr group on day 3 (7.2 [5.2; 10.5] vs 10.0 [9.7; 13.2], $P=0.045$) and day 7 (8.0 [7.3; 9.2] vs 10.0 [9.0; 11.5], $P=0.027$) (Fig. 1).

MRI examination of the brain. Based on MRI findings, the average volume of damage in the Ischemia + iAr group and the Ischemia group was 12.5 [8.5; 17.4] mm³ and 21.0 [17.5; 22.68] mm³, respectively. Statistically significant differences were found between the groups ($P=0.01$) (Fig. 2).

Histochemical assessment of ischemic brain damage. Nissl staining showed that the lesions were distinct and clearly demarcated from the surrounding area of the ischemic focus. The underlying white matter was partially affected. The newly formed barrier in the form of a glial scar was more definite in the Ischemia + iAr group. Also in the Ischemia + iAr group, full-blooded capillaries with endotheliocytes were identified, as well as abundant fibroblasts in the cellular infiltration zone. In the Ischemia group, there were practically no capillaries, and heterogeneous neurons (dark, with a hyperchromic nucleus, displaced nucleus and/or nucleolus) were identified in the penumbra zone (Fig. 3, *a*). A significantly smaller average width of the penumbra was found in the Ischemia + iAr group ($P=0.039$).

Immunohistochemical analysis of histological sections of the brain. According to the literature, NeuN can be located both in the nuclei of neurons and in the cytoplasm [22, 23]. NeuN-positive cells were found in the area of ischemic damage in both groups. However, in the penumbra zone, the number of NeuN-positive cells was significantly higher in the Ischemia + iAr group (Ischemia group 43 [35; 46], vs. Ischemia + iAr group 60 [51; 73], $P=0.042$) (Fig. 3, *d*). Outside the ischemic lesion, the number of NeuN-positive cells was also significantly higher in the Is-

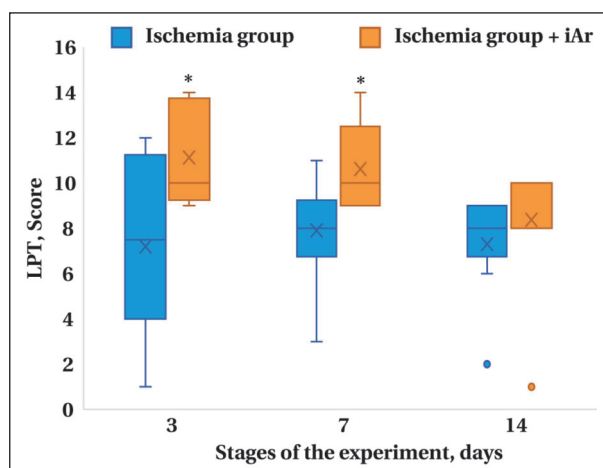


Fig. 1. LPT test. LPT test results on days 3, 7, and 14 after ischemia modeling.

Note. * — statistically significant differences between the Ischemia and Ischemia + iAr groups. Data are presented as medians and quartiles [25%; 75%]. The ANOVA test was used to compare three or more groups.

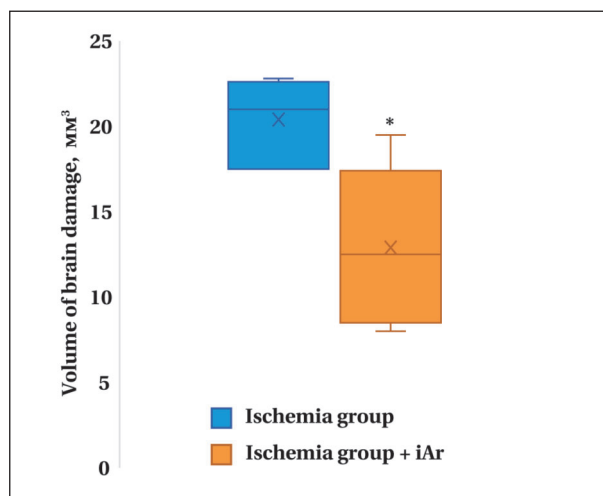


Fig. 2. Volume of brain damage on the 14th day of observation.

Note. Data are presented as medians and quartiles [25%; 75%]. * — statistically significant differences between groups.

Table 1. Sequences and main characteristics of primers used for real-time PCR.

Gene	Organism	Primer sequences (forward and reverse), 5'-3'	Annealing temperature, °C
18SrRNA	Rat	GACAGGATTGACAGATTGAT	56
		TTATCGGAATTAACCAGACAA	
TNF	Rat	TTATCTACTCCCAGGTCT	56
		TGGTATGAAATGGCAAATC	
IL-1beta	Rat	AGAACATAAGCCAACAAGT	56
		ACACAGGACAGGTATAGAT	
IL-6	Rat	TGATTGTATGAACAGCGATGATG	58
		CCAGAAGACCAGAGCAGATT	

Table 2. Real time PCR protocol.

Period	Time	Temperature, °C	Number of cycles
Initiation	5 min	95	1
Denaturation	1 min	95	45
Denaturation	20 s	See Table 1	
Elongation	20 s	72	
	1 min	72	1
Obtaining the melting curve	30 s	Every 30 s the temperature increases by 0.5°C	45

chemia + iAr group, i. g. 250 [215; 353] cells in the Ischemia + iAr group vs 150 [45; 200] cells in the Ischemia group ($P=0.043$). Iba1 is a marker of microglia/macrophages [24–26]. A larger area occupied by Iba-1-positive cells was found in the Ischemia group compared to the Ischemia + iAr group ($P=0.037$). We could not differentiate these cells from systemic macrophages (Fig. 3, *b*). The area of vWF-positive staining in the Ischemia + iAr group was statistically significantly greater than in the control group, 0.23 [0.20; 0.29] vs. 0.15 [0.14; 0.18] ($P=0.034$). Quantitative analysis of Cas-3-positive cells showed a decrease in Cas-3-positive cells count in the Ischemia + iAr group compared to the Ischemia group, but the differences were not significant (Fig. 3, *c*).

Assessment of IL-1 β , IL-6, and TNF mRNA content in the brain. Table 2 shows (real-time PCR data for IL-1 β mRNA, IL-6 mRNA, and TNF mRNA in the rat brain homogenates after photo-induced brain ischemia modeling and treatment with Argox. The study revealed that the relative amount of IL-1 β mRNA and TNF mRNA was significantly lower after exposure to an argon-oxygen mixture. Analysis of relative IL-6 mRNA amounts showed no significant difference between the groups. For the first time, it was shown that three 60-minute inhalations of an argon-oxygen mixture (Ar 70%/O₂ 30%) after ischemic stroke exhibit neuroprotective properties due to their effect on cellular response. The model of ischemic stroke induced via occlusion of the middle cerebral artery is the most commonly used in experimental studies, but this method has limitations [1]. The photochemical thrombosis method is a relatively simple, reproducible model with minimal limitations and complications [27].

The only potential target for neuroprotective agents is the penumbra zone, involving cell response within and around it [28–30]. Our study showed that three 60-minute inhalations of argon-oxygen mixture in a photo-induced ischemic stroke model leads to a significant reduction in neurological deficit, a decrease in the volume of damage according to MRI findings, and a decrease in the average width of the penumbra according to histological findings. There are few studies that investigated the effect of argon-oxygen mixture on the models of photo-induced ischemic stroke using the immunohistochemical method. In this study, the effect of argon-oxygen mixture on microglia, neurons, apoptotic processes and angiogenesis processes was evaluated.

During a stroke or traumatic brain injury, massive neurons death occurs, partly caused by apoptotic processes. In oxygen and glucose deficiency, apoptosis pathways are activated, leading to widespread disruption of the nervous tissue structure and function. The extent of neuronal damage during ischemia is a crucial factor in determining the outcome. Oxidative

stress, excitotoxicity, and cellular responses contribute to neuronal damage [28]. It was shown that the activity of apoptosis processes significantly decreases after exposure to an argon-oxygen mixture, as indicated by the dynamics of neuronal caspase-3 (Cas-3) content. Microglia plays a crucial role in cell proliferation and formation of glial scars after ischemic damage. It is also a source of pro- and anti-inflammatory agents in the brain [31]. Iba-1 staining was used to study microglia, as Iba-1 is a marker for microglia/macrophages [9, 10].

Published studies [9, 10] report that the number of Iba-1+ cells peaked 4 days after ischemia and remained high after 8 days. A statistically significant decrease in the density of Iba-1-positive cells in the Ischemia + iAr group was shown, which suggests that microglia activity is reduced by the end of the second week after exposure to the argon-oxygen mixture. This is also supported by the statistically significant low level of Cas-3-positive cells. Identification of the type of macrophages seems to be very challenging. Microglia activation and increased capacity for phagocytosis occur in the first 24 hours after a stroke [9, 10].

Subsequently, it remains difficult to discern the identified macrophages as systemic, as the ischemic process leads to breakdown of the blood-brain barrier and release of macrophages from the vascular system [9, 10]. Specific neuronal markers, such as neuron-specific enolase, neurofilament proteins, and calbindin are used to differentiate neurons from glial cells in brain sections. NeuN protein is a splicing regulator. In this study, the number of NeuN-positive cells was significantly higher in the group receiving argon-oxygen inhalation. These data may indicate a greater number of preserved neurons in the damaged and the penumbra area, however, we cannot appreciate the functionality of these neurons.

Fahlenkamp et al. demonstrated that argon affects microglia activation in an in vitro model of LPS-induced inflammation in microglia cell cultures [31–33]. The results of these studies showed that argon suppresses the expression of the pro-inflammatory IL-1 β gene. Another group of authors using a model of oxygen-glucose deprivation in cortical neuronal cell cultures showed that argon exposure reduces neuronal cell death by decreasing the expression of pro-inflammatory cytokines TNF- α and IL-6 [33]. Interleukins play a reversing role in ischemic damage by transmitting information, activating, and regulating immune cells. They also affect the activation, proliferation, and differentiation of T and B cells, as well as the activity of cellular responses that involve the expression of pro-inflammatory mediators [11]. In this study, the use of argon resulted in a statistically significant reduction in the expression of IL-1 β and TNF- α genes. IL-1

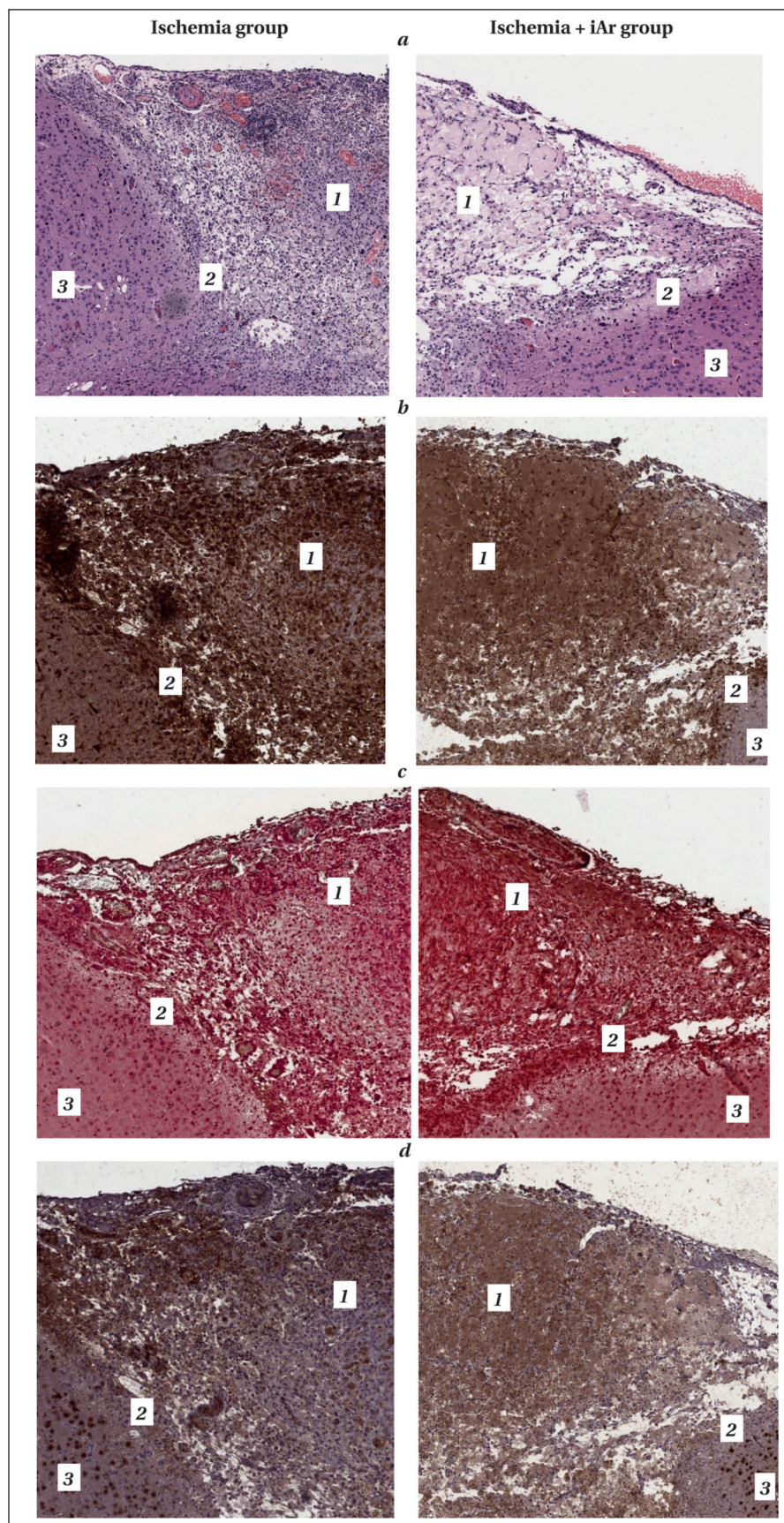


Fig. 3. Representative images of histological micro-preparations of rat brain.
Note. 1 — lesion; 2 — penumbra; 3 — undamaged tissue. *a* — stained with hematoxylin and eosin, $\times 20$ magnification; *b* — Iba-1 staining, $\times 20$ magnification; *c* — combined staining for von Willebrand factor (vWF): cells are stained red and caspase-3 (Cas-3) is stained brown; *d* — NeuN-positive cells.

can cause neurotoxicity indirectly through its action on vascular endothelium, promoting the recruitment of leukocytes, particularly neutrophils, which damage the neurovascular unit by releasing MMPs and reactive oxygen species (ROS) [11]. However, in the subacute and chronic phases after stroke, some effects of IL-1 may be beneficial. For example, IL-1 promotes glial scar formation and enhances angiogenesis, thereby contributing to recovery after ischemic stroke [11]. IL-1 β is a member of the IL-1 family. Given that the expression level of the IL-1 β gene was found to be above the normal values, its positive effect on the formation of scar tissue and new capillaries can be assumed, as evidenced by the large area of vWF-positive staining in the Ischemia + iAr group.

However, on the other hand, some studies have shown that IL-1 β can influence the activation of the PI3K/AKT pathway, resulting in the production of IL-6 and other cytokines that affect ischemic areas and exacerbate the damage, activating apoptosis processes [11]. Nonetheless, when compared with the Ischemia group, the expression of the IL-1 β gene was statistically significantly lower after exposure to the argon-oxygen mixture, indicating that its apoptotic effect was weaker than that of the oxygen-nitrogen mixture, as evidenced by the low number of Cas-3 positive cells in the Ischemia + iAr group. The results of this study showed that the IL-6 gene expression levels in the Ischemia + iAr group did not differ significantly from that in the Ischemia group. Some studies have shown that IL-6 favors neuronal survival in the central nervous

system by reducing excitotoxic and NMDA-mediated damage to neurons, and by protecting neurons from apoptosis [12]. IL-6 demonstrates a dual effect in ischemic stroke, acting as a factor in the acute stage and as a neurotrophic mediator in the subacute and chronic phase [11, 12, 34, 35]. Thus, the argon-oxygen mixture in the model of photo-induced ischemic stroke reduces the severity of neurological deficit, decreases the lesion size according to MRI findings, reduces the expression level of pro-inflammatory cytokine genes, and also affects the cellular response according to histological and immunohistochemical findings.

Limitations of the study. One of the main limitations of the study was the use of chloral hydrate as an anesthetic during the ischemic stroke modeling stage because of limited choice of anesthetics as allowed by a local law. Other limitations include the relatively small number of animals in the groups, especially in the sham-operated group, which reduced the statistical power in several comparisons. Additionally, the study did not include a functional analysis of neuronal circuit preservation or an assessment of behavioral cognitive functions to further confirm the effectiveness of argon-oxygen therapy in a pre-clinical setting.

Conclusion

Three 60-minute inhalations of an argon-oxygen mixture (Ar 70%/O₂ 30%) reduced the severity of neurological deficits in animals after ischemic stroke by influencing the cellular responses in the lesion and penumbra.

References

- Ostrova I. V., Babkina A. S., Lyubomudrov M. A., Grechko A. V., Golubev A. M. Применение фотохимического тромбоза для моделирования ишемического инсульта (обзор). *Общая реаниматология*. 2023; 19 (3): 54–65. Ostrova I. V., Babkina A. S., Lyubomudrov M. A., Grechko A. V., Golubev A. M. Photochemically induced thrombosis as a model of ischemic stroke (review). *General Reanimatology = Obshchaya Reanimatologiya*. 2023; 19 (3): 54–65. (in Russ.&Eng.). DOI: 10.15360/1813-9779-2023-3-54-65.
- Cipriani R., Domerq M., Martín A., Matute C. Role of microglia in stroke. *Adv Neurobiol*. 2024; 37: 405–422. DOI: 10.1007/978-3-031-55529-9_23. PMID: 39207705.
- Bitar L., Puig B., Oertner T. G., Dénes Á., Magnus T. Changes in neuroimmunological synapses during cerebral ischemia. *Transl Stroke Res*. 2024. DOI: 10.1007/s12975-024-01286-1. PMID: 39103660.
- Grinchevskaya L. R., Salikhova D. I., Silachev D. N., Goldshtein D. V. Neural and glial regulation of angiogenesis in CNS in ischemic stroke. *Bull Exp Biol Med*. 2024. DOI: 10.1007/s10517-024-06219-4. PMID: 39266920.
- Hakon J., Quattromani M. J., Sjölund C., Talhada D., Kim B., Moyanova S., Mastroiacovo F., et al. Inhibiting metabotropic glutamate receptor 5 after stroke restores brain function and connectivity. *Brain*. 2024; 4; 147 (1): 186–200. DOI: 10.1093/brain/awad293. PMID: 37656990.
- Takahashi S. Metabolic contribution and cerebral blood flow regulation by astrocytes in the neurovascular unit. *Cells*. 2022; 11 (5): 813. DOI: 10.3390/cells11050813. PMID: 35269435.
- Pinto M. J., Ragozzino D., Bessis A., Audinat E. Microglial modulation of synaptic maturation, activity, and plasticity. *Adv Neurobiol*. 2024; 37: 209–219. DOI: 10.1007/978-3-031-55529-9_12. PMID: 39207694.
- Guffart E., Prinz M. Evolution of microglia. *Adv Neurobiol*. 2024; 37: 39–51. DOI: 10.1007/978-3-031-55529-9_3. PMID: 39207685.
- Knezic A., Budusan E., Saez N. J., Broughton B. R. S., Rash L. D., King G. F., Widdop R. E., et al. Hila improves sensorimotor deficit following endothelin-1-induced stroke in rats but does not improve functional outcomes following filament-induced stroke in mice. *ACS Pharmacol Transl Sci*. 2024; 7 (4): 1043–1054. DOI: 10.1021/acspsci.3c00328. PMID: 38638162.
- Jia J., Yang L., Chen Y., Zheng L., Chen Y., Xu Y., Zhang M. The role of microglial phagocytosis in ischemic stroke. *Front Immunol*. 2022; 12: 790201. DOI: 10.3389/fimmu.2021.790201. PMID: 35082781.
- Zhu H., Hu S., Li Y., Sun Y., Xiong X., Hu X., Chen J., et al. Interleukins and ischemic stroke. *Front Immunol*. 2022; 13: 828447. DOI: 10.3389/fimmu.2022.828447. PMID: 35173738.
- Yuan S., Lin A., He Q. Q., Burgess S., Larsson S. C. Circulating interleukins in relation to coronary artery disease, atrial fibrillation and ischemic stroke and its subtypes: a two-sample Mendelian randomization study. *Int J Cardiol*. 2020; 313: 99–104. DOI: 10.1016/j.ijcard.2020.03.053. PMID: 32223966.
- Kong X., Gong Z., Zhang L., Sun X., Ou Z., Xu B., Huang J., et al. JAK2/STAT3 signaling mediates IL-6-inhibited neurogenesis of neural stem cells through DNA demethylation/methylation. *Brain Behav Immun*. 2019; 79: 159–173. DOI: 10.1016/j.bbi.2019.01.027.
- Jurcau A., Ardelean A. I. Oxidative stress in ischemia/reperfusion injuries following acute ischemic stroke. *Biomedicines*. 2022; 10 (3): 574. DOI: 10.3390/biomedicines10030574. PMID: 35327376.
- Zhu H., Jian Z., Zhong Y., Ye Y., Zhang Y., Hu X., Pu B., et al. Janus kinase inhibition ameliorates ischemic stroke injury and neuroinflammation through reducing NLRP3 inflammasome activation via JAK2/STAT3 pathway inhibition. *Front Immunol*. 2021; 12: 714943. DOI: 10.3389/fimmu.2021.714943. PMID: 34367186.
- Боева Е. А., Гребенчиков О. А. Органопротективные свойств аргона (обзор). *Общая реаниматология*. 2022; 18 (5): 44–59. Boeva E. A., Grebenchikov O. A. Organoprotective properties of argon (review). *General Reanimatology = Obshchaya Reanimatologiya*. 2022; 18 (5): 44–59. (in Russ.&Eng.). DOI: 10.15360/1813-9779-2022-5-44-59.
- Боева Е. А., Силачев Д. Н., Якупова Э. И., Милованова М. А., Варнакова Л. А., Калабушев С. Н., Денисов С. О., с соавт. Изучение нейропротективного эффекта ингаляции аргон-кислородной смеси после фотоиндуцированного ишемического инсульта. *Общая реаниматология*. 2023; 19 (3): 46–53. Boeva E. A., Silachev D. N., Yakupova E. I., Milovanova M. A., Varnakova L. A., Kalabushev S. N., Denisov S. O. et al. Experimental study of neuroprotective properties of inhaled argon-oxygen mixture in a photoinduced ischemic stroke model. *General Reanimatology = Obshchaya Reanimatologiya*. 2023; 19 (3): 46–53. (in Russ.&Eng.). DOI: 10.15360/1813-9779-2023-3-46-53.
- Бочарников А. Д., Боева Е. А., Милованова М. А., Антонова В. В., Якупова Э. И., Гречко А. В. Оценка нейропротективных свойств анестетиков на моделях повреждения мозга. *Общая реаниматология*. 2024; 20 (2): 65–69. Bocharnikov A. D., Boeva E. A., Milovanova M. A., Antonova V. V., Yakupova E. I., Grechko A. V. Neuroprotection by anesthetics in brain injury models. *General Reanimatology = Obshchaya Reanimatologiya*. 2024; 20 (2): 65–69. (in Russ.&Eng.). DOI: 10.15360/1813-9779-2024-2-65-69.
- Silachev D. N., Uchevatkin A. A., Pirogov Y. A., Zorov D. B., Isaev N. K. Comparative evaluation of two methods for studies of experimental focal ischemia: magnetic resonance tomography and triphenyltetrazoleum detection of brain injuries. *Bull Exp Biol Med*. 2009; 147 (2): 269–272. DOI: 10.1007/s10517-009-0489-z.
- De Ryck M., Van Reempts J., Borgers M., Wauquier A., Janssen P. A. Photochemical stroke model: flunarizine prevents sensorimotor deficits after neocortical infarcts in rats. *Stroke*. 1989; 20 (10): 1383–1390. DOI: 10.1161/01.str.20.10.1383.
- Jolkkonen J., Puurunen K., Rantakömi S., Härkönen A., Haapalinna A., Sivenius J. Behavioral effects of the

- alpha (2)-adrenoceptor antagonist, atipamezole, after focal cerebral ischemia in rats. *Eur J Pharmacol.* 2000; 400 (2–3); 211–219.
DOI: 10.1016/s0014-2999 (00)00409-x.
22. Anderson M. B., Das S., Miller K. E. Subcellular localization of neuronal nuclei (NeuN) antigen in size and calcitonin gene-related peptide (CGRP) populations of dorsal root ganglion (DRG) neurons during acute peripheral inflammation. *Neurosci Lett.* 2021; 760: 135974. DOI: 10.1016/j.neulet.2021.135974.
 23. Zhu X., Yi Z., Li R., Wang C., Zhu W., Ma M., Lu J., Li P. Constructing a transient ischemia attack model utilizing flexible spatial targeting photothrombosis with real-time blood flow imaging feedback. *Int J Mol Sci.* 2024; 25 (14): 7557. DOI: 10.3390/ijms25147557. PMID: 39062800.
 24. Villa-González M., Rubio M., Martín-López G., Mallavibarrena P. R., Vallés-Saiz L., Vivien D., Wandosell F., et al. Pharmacological inhibition of mTORC1 reduces neural death and damage volume after MCAO by modulating microglial reactivity. *Biol Direct.* 2024; 19 (1): 26. DOI: 10.1186/s13062-024-00470-5. PMID: 38582839.
 25. Koukalova L., Chmelova M., Amlerova Z., Vargova L. Out of the core: the impact of focal ischemia in regions beyond the penumbra. *Front Cell Neurosci.* 2024; 18: 1336886. DOI: 10.3389/fncel.2024.1336886. PMID: 38504666.
 26. Chiang P. T., Tsai H. H., Yen R. F., Tsai Y. C., Wu C.H., Chiu C. H., Tsai L. K. *in vivo* detection of poststroke cerebral cell proliferation in rodents and humans. *Ann Clin Transl Neurol.* 2024; 11 (2): 497–507. DOI: 10.1002/acn3.51972.
 27. Chen W., Zhang Y., Yin M., Cheng Z., Li D., Luo X., Liu X., et al. Circular R. NA circPRDX3 mediates neuronal survival apoptosis in ischemic stroke by targeting miR-641 and NPR3. *Brain Res.* 2022; 1797: 148114. DOI: 10.1016/j.brainres.2022.148114.
 28. Kanemura Y., Yamamoto A., Katsuma A., Fukusumi H., Shofuda T., Kanematsu D., Handa Y., et al. Human-induced pluripotent stem cell-derived neural progenitor cells showed neuronal differentiation, neurite extension, and formation of synaptic structures in rodent ischemic stroke brains. *Cells.* 2024; 13 (8): 671. DOI: 10.3390/cells13080671. PMID: 38667286.
 29. Boyle B. R., Berghella A. P., Blanco-Suarez E. Astrocyte regulation of neuronal function and survival in stroke pathophysiology. *Adv Neurobiol.* 2024; 39: 233–267. DOI: 10.1007/978-3-031-64839-7_10. PMID: 39190078.
 30. Krenzlin H., Wesp D. M.A., Korinek A. A.E., Ubbens H., Volland J., Masomi-Bornwasser J., Weber K. J., et al. Effects of argon in the acute phase of subarachnoid hemorrhage in an endovascular perforation model in rats. *Neurocrit Care.* 2024. DOI: 10.1007/s12028-024-02090-3. PMID: 39174846.
 31. Moulson A. J., Squair J. W., Franklin R. J.M., Tetzlaff W., Assinck P. Diversity of reactive astrogliosis in CNS pathology: heterogeneity or plasticity? *Front Cell Neurosci.* 2021; 15: 703810. DOI: 10.3389/fncel.2021.703810. PMID: 34381334.
 32. Takamatsu H., Tatsumi M., Nitta S., Ichise R., Muramatsu K., Iida M., Nishimura S., et al. Time courses of progress to the chronic stage of middle cerebral artery occlusion models in rats. *Exp Brain Res.* 2002; 146 (1): 95–102. DOI: 10.1007/s00221-002-1147-0. PMID: 12192583.
 33. Qin C., Zhou L. Q., Ma X.T., Hu Z.W., Yang S., Chen M., Bosco D. B., et al. Dual functions of microglia in ischemic stroke. *Neurosci Bull.* 2019; 35 (5): 921–933. DOI: 10.1007/s12264-019-00388-3.
 34. Силкин В. В., Ершов В. И., Бурдаков В. В., Бирюкова Т. В., Бредихин А. Ю., Лозинская Т. Ю. Математическое моделирование тяжелого ишемического инсульта с полиорганной недостаточностью: ретроспективное наблюдательное исследование. *Вестник интенсивной терапии имени А. И. Салтанова.* 2023; (1): 91–100. Silkin V. V., Yershov V. I., Burdakov V. V., Biryukova T. V., Bredikhin A. Yu., Lozinskaya T. Yu. Mathematical modeling of severe ischemic stroke with multiple organ failure: a retrospective observational study. *Ann Crit Care = Vestnik Intensivnoy Terapii im A. I. Saltanova.* 2023; (1): 91–100. (in Russ.). DOI: 10.21320/1818-474X-2023-1-91-100.
 35. Авидзба А. Р., Саскин В. А., Киров М. Ю. Гемодинамика и реперфузионная терапия при ишемическом инсульте: друзья или враги? *Анестезиология и реаниматология.* 2024; (2): 91–96. Avidzba A. R., Saskin V. A., Kirov M. Y. Hemodynamics and reperfusion in ischemic stroke: friends or foes? *Russ J Anesthesiol. Reanimatol = Anesteziologiya i Reanimatologiya.* 2024; (2): 91–96. DOI: 10.17116/anaesthesiology202402191.

Received 07.11.2024

Accepted 29.04.2025

Online first 03.06.2025